

# LASER SINTERING OF STAINLESS STEEL USING RESIN POWDER

Y. Imai\*, H. Kyogoku\*\* and K. Shiraishi\*\*\*

\*Graduate School, Kinki University

\*\*Department of Mechanical Engineering, Kinki University

\*\*\*Department of Biotechnology and Chemistry, Kinki University  
Higashihiroshima, Hiroshima 739-2116 Japan

## Abstract

We tried laser sintering of 316L stainless steel powder using resin powder. The laser sintering conditions such as laser power, scan speed and scan pitch with a YAG laser, and the influence of additional resin powder on the density and the tensile properties of the sintered alloy were investigated experimentally. The tensile specimen was laser-sintered with a YAG laser, and then debound and sintered in a vacuum furnace. The tensile specimen was successfully fabricated. The relative density and the tensile strength varied with the additional resin powder, and the optimum weight percentage of additional resin powder was around 4%. The relative density of the sintered alloy was approximately 85%, and the tensile strength and elongation of the sintered alloy were more than 280 MPa and 15% respectively.

## Introduction

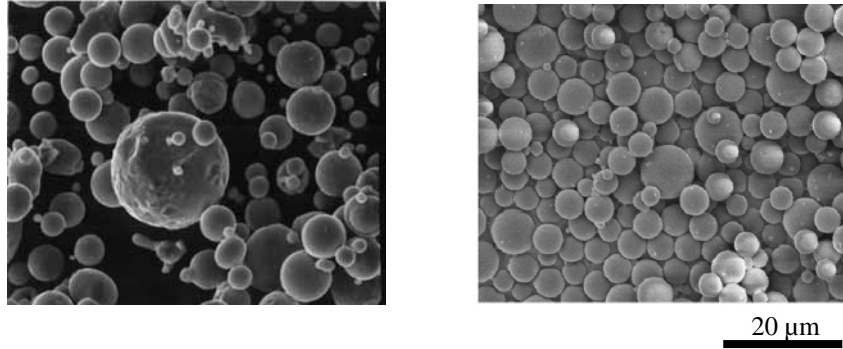
Selective laser sintering is a rapid prototyping process which can produce complex-shape parts directly from metals and ceramics powders, and this process has been applied to fabricate various parts, molds and so on[1-3]. This process is generally divided into indirect and direct selective laser sintering. In the case of indirect selective laser sintering, a polymer coated powder is used, and therefore the selection of materials is considerably limited and a post-sintering process is needed. On the other hand, in the case of direct selective laser sintering, since a mixture of metal or ceramics powders is used, this process is applicable to various alloy system but the appropriate amount of flow is critical due to liquid-phase sintering [4]. In the case of the former, if an appropriate polymer powder can be used without segregation, this process can be widely applied to various alloy systems. There are some papers on the laser sintering of stainless steel such as 316L and 17-4 PH[5,6], and stainless steel has been commercially used in the field of laser sintering.

In this study, we tried laser sintering 316L stainless steel powder using a polyamide resin powder with a YAG laser. The laser sintering conditions were examined experimentally, and the influence of the weight ratio of the binder on the density, microstructure and tensile properties of the sintered specimens were also investigated.

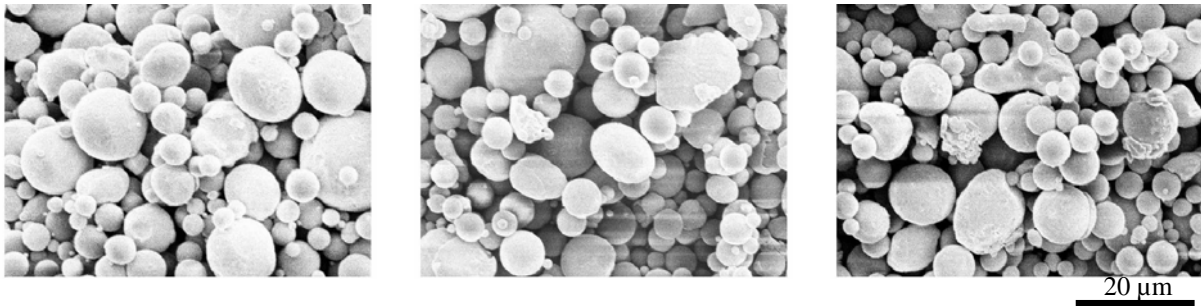
## Experimental Method

### Powders

In this study, we used a gas-atomized 316L stainless steel powder and a polyamide resin powder as a binder. The mean particle diameters of the stainless steel powder and the resin powder were 9  $\mu\text{m}$  and 6  $\mu\text{m}$ . Both powders are spherical in shape, as shown in Fig.1. These powders were blended at a weight ratio between the stainless steel powder and the resin powder from 100:3 to 100:10. Figure 2 shows the mixing state in various mixtures of 316L stainless steel and polyamide resin powder. Both powders were mixed homogeneously, as shown in Fig.2. It is very important to obtain a homogeneous mixture in order to avoid segregation during laser sintering. The mixtures were filled into an aluminum die and then laser-sintered with a YAG laser equipment.



(a) 316L stainless steel powder (b) Resin powder  
 Fig.1 Shape of 316L stainless steel powder and resin powder



(a) 100:3 (b) 100:4 (c) 100:5  
 Fig.2 Mixing state in various mixtures of stainless steel powder and resin powder

**Experimental procedure**

The laser beam was focused down on a diameter 0.85 mm spot. The scan speed was changed from 1.67 mm/s to 10 mm/s, and the scan pitch was changed from 0.4 mm to 0.85 mm. The scan speed and scan pitch were numerically controlled by a XY table. The laser power measured was 34 W on the surface of the powder bed. Figure 3 shows the schematic diagram of this setup. We used 9 aluminum sheets, on each of which we curved out a rectangular trough. The powder was then manually compacted between each of the rectangular trough. The powder surface was then leveled so that it matched the focal position of the laser beam. The laser-sintered body obtained was debound at 573 K for 7.2 ks, and then sintered at 1623 K for 3.6 ks in a vacuum furnace.

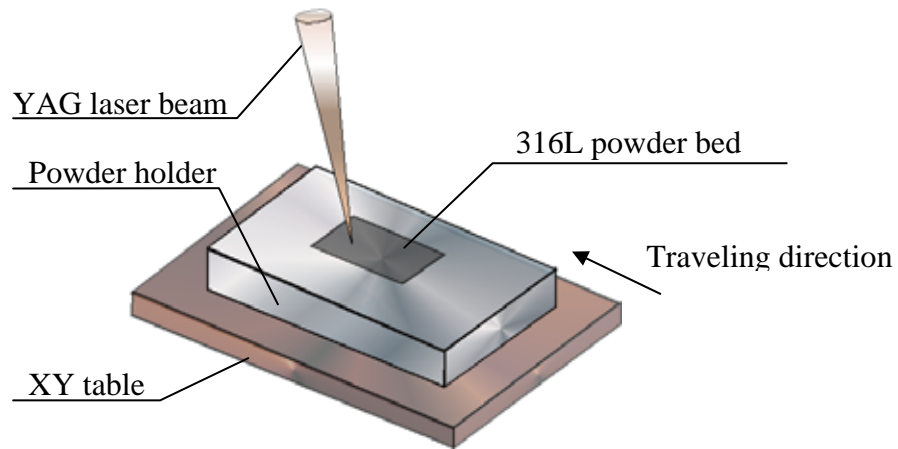


Fig. 3 Schematic diagram of the laser sintering

The density of the specimen was measured by a fluid immersion (Archimedes) method. The microstructure of the specimen was examined by an optical microscope and a scanning electron microscope with EDX. Microscopical observations were made after being etched electrically in 10% oxalic acid solution. Tensile tests were performed by an Instron tensile testing machine with a cross-head rate of  $1.67 \times 10^{-5}$  m/s.

## Results and Discussions

### Laser sintering conditions on the shape and surface state of scan tracks

It is significant to investigate the laser sintering conditions, such as laser power, scan speed and scan pitch, in order to fabricate superior laser-sintered bodies. Therefore, we investigated the effects of laser power and scan speed on the shape and surface state of scan tracks. Figure 4 shows the change in shape of single-scan tracks with scan speed. The width of a single-scan track decreases by increasing the scan speed and becomes approximately constant in scanning direction, as shown in Fig.4(c). Figure 5 shows the surface morphology of a single-scan track. Surface ripples which provide a smoother surface are observed, but the “balling” effect is hardly observed. As a result, the continuous columnar shape of a scan track and the fairly smooth surface of a scan track could be obtained at a scan speed of 10 mm/s. Figure 6 shows the morphology of a laser-sintered body. The polyamide resin powder is only melted during the laser sintering process and the melted polymer bonds together the stainless steel powder, as shown in Fig.6. Thus the laser-sintered body is in a state fabricated by an indirect laser sintering process.

Figure 7 shows the change in the surface state of the laser-sintered body with a scan pitch. In the case of a narrower scan pitch, the surface of the laser-sintered body becomes round in shape during the melting-solidification phenomenon. This may be because the powder absorbed a large amount of energy due to a narrower scan pitch. On the other hand, in the case of a wider scan pitch, overlapping a smaller area, the surface of the laser-sintered body shows apparently wider scan tracks as shown in Fig.7(c). This means that the bonding among the adjacent scan tracks is poor. As a result, the fairly smooth surface of the laser-sintered body could be obtained at a scan pitch of around 0.6 mm (Fig.7 (b)).

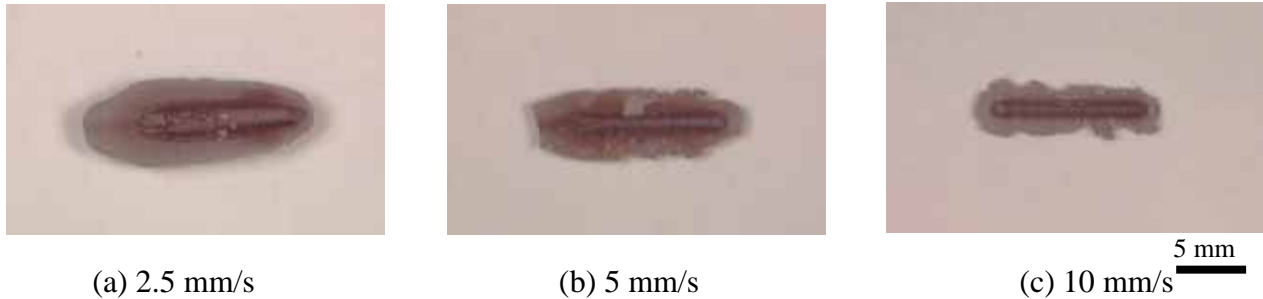


Fig.4 Change in shape of single-scan tracks with scan speed

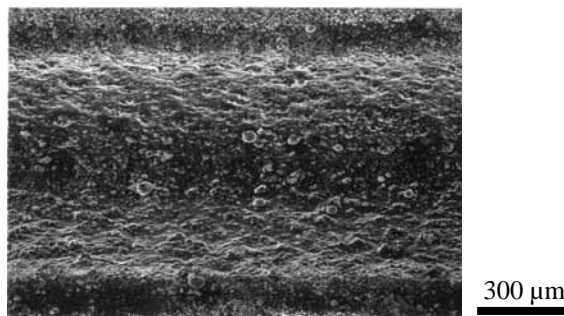


Fig.5 An example of the surface morphology of single-scan track (10 mm/s, 34 W)

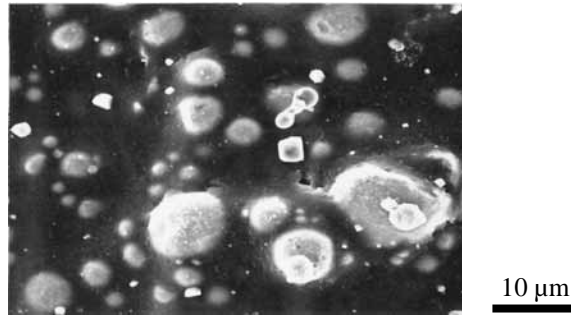


Fig.6 Morphology of laser-sintered body

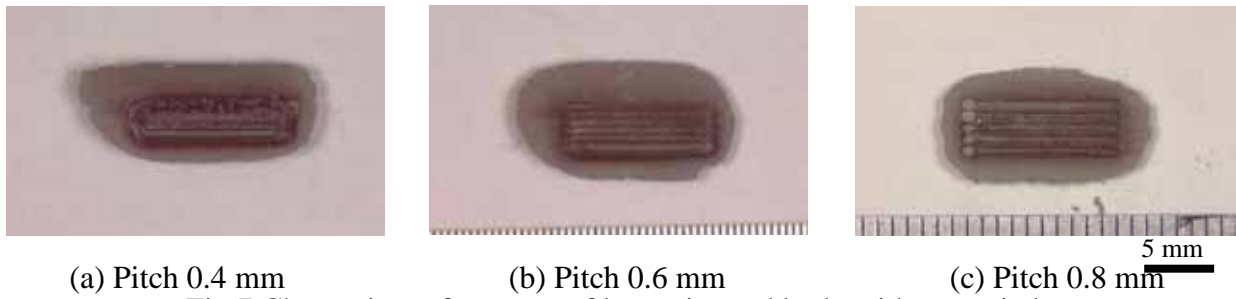


Fig.7 Change in surface state of laser-sintered body with scan pitch

**Influence of the weight ratio of the binder on the density and microstructure of sintered body**

Figure 8 shows the variation in relative density of the sintered body as a function of the weight ratio of the binder (resin powder). The relative density is approximately constant at a weight ratio from 3 to 5, but it lowers at a weight ratio of the binder more than 5. Thus it was found that the optimum weight ratio of the binder is around 4.

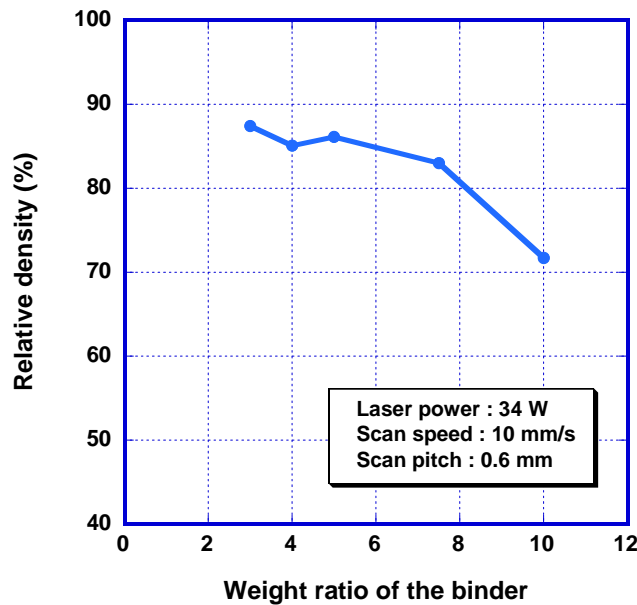


Fig.8 Variation in relative density of the sintered body as a function of the weight ratio of the binder

Figure 9 shows the variation in microstructure of the sintered body as a function of the weight ratio of the binder. According to the Schaeffler diagram [7], the microstructure of the sintered body consists of austenite phase. The grain size increases with increasing the weight ratio of the binder. In the case of a weight ratio of 7.5, the grain size becomes larger, and large pores form. As already reported [8], in the case of a stainless steel body fabricated by metal injection molding method, the microstructure changes with an increasing in carbon content. The grain size increases and the density decreases. Figure 10 shows the variation in carbon content of the sintered body as a function of the weight ratio of the binder. The carbon content increases with increasing the weight ratio. The change in microstructure of the sintered body corresponds to that in carbon content. The carbon content of the sintered body is the minimum value of 0.015% at a weight ratio of 4. This carbon content satisfies the standard (AISI) value of chemical compositions. Thus it was found that optimum results in density and microstructure were obtained at a weight ratio of 4.

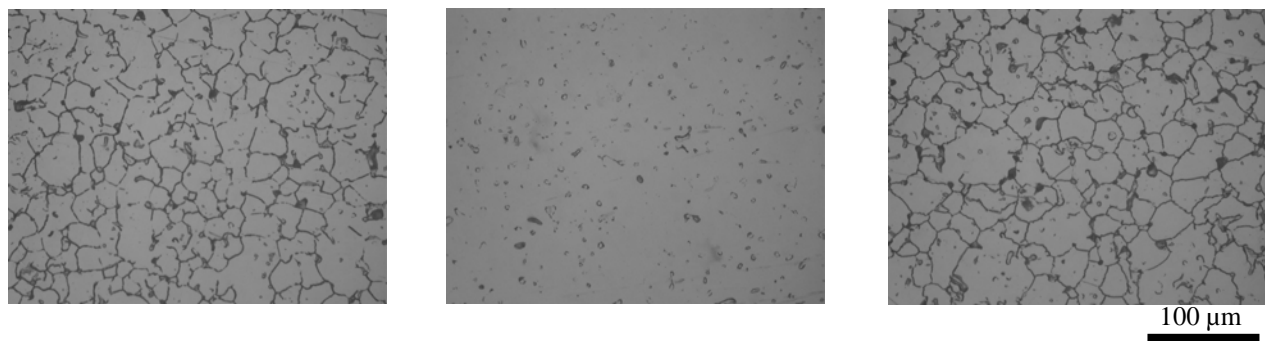


Fig.9 Variation in microstructure of the sintered body as a function of the weight ratio of the binder

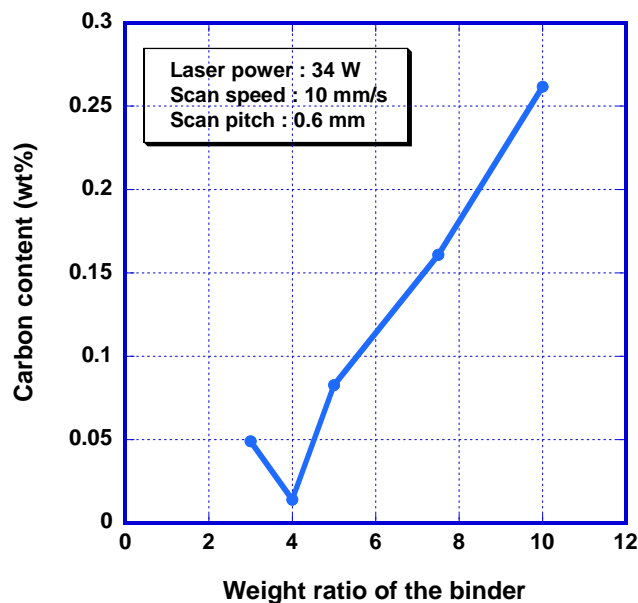
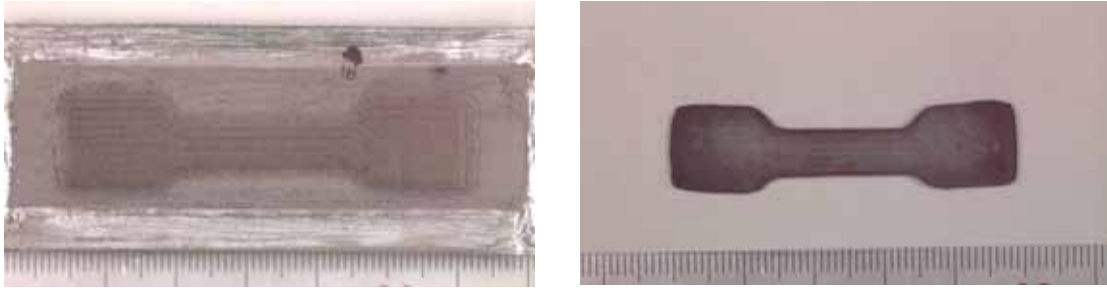


Fig.10 Variation in carbon content of the sintered body as a function of the weight ratio of the binder

### Tensile properties of sintered body

The tensile specimen was fabricated as shown in Fig.11. The laser-sintered body and the sintered body at a weight ratio of 4 are given in Fig.11 (a) and (b) respectively. The tensile test was performed using the sintered body. Tensile properties of the sintered bodies at various weight ratios are given in Table 1. The stress-strain curve of the sintered body at a weight ratio of 4 is given in Fig.12. It is found from this result that the tensile strength and elongation are 280MPa and 15% respectively. Compared with the MPIF standards for metal injection molded parts, the tensile strength and elongation of the sintered body are rather lower than those of the standard (450 MPa and 40%, respectively). This is probably because the bonding among the adjacent layers is poor as shown in Fig.13.



(a) Laser-sintered body (b) Sintered body  
Fig.11 Tensile specimen of the laser-melted body and the sintered body

Table 1 Tensile properties of sintered bodies

Weight ratio of the binder	Tensile strength (MPa)	Elongation (%)
100 : 3	230	15.7
100 : 4	282	15.2
100 : 5	186	10.6
MPIF standard	450	40

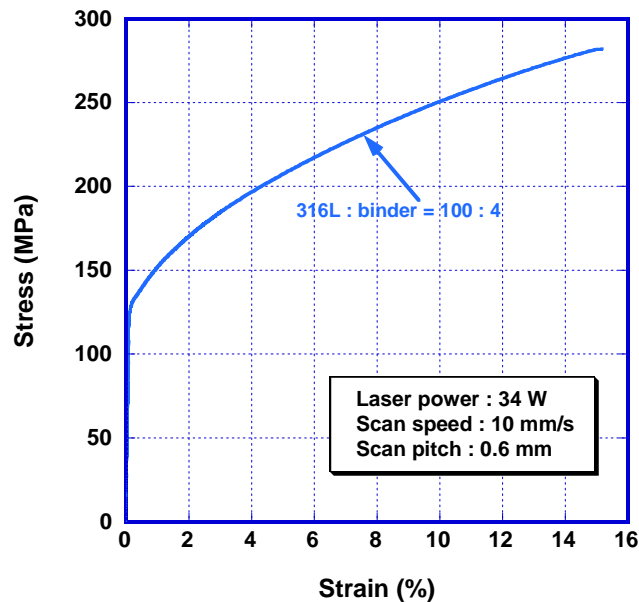
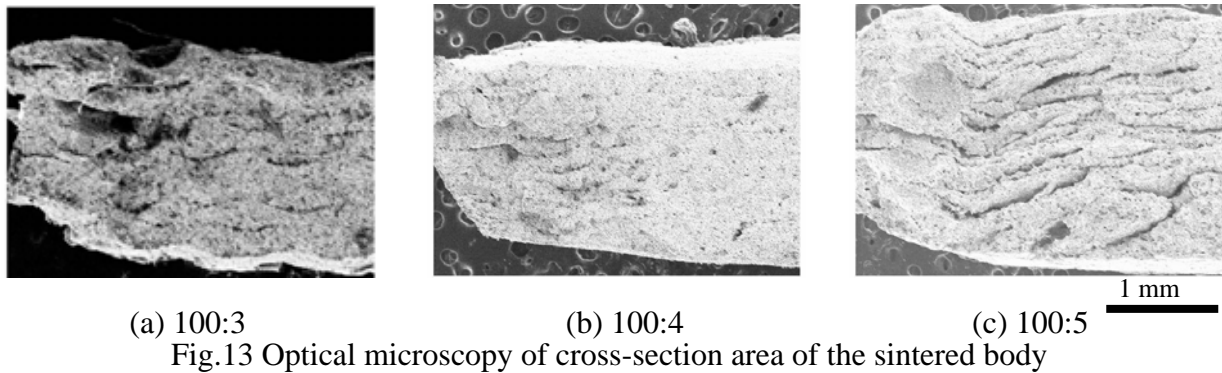


Fig.12 An example of stress-strain curve of the sintered body



### Conclusions

In this study, we tried laser sintering of 316L stainless steel with a YAG laser. The laser sintering conditions were examined experimentally, and the influence of the weight ratio of the binder on the density, microstructure and tensile properties of the sintered specimens were also investigated. The results obtained are as follows:

- (1) The laser-sintered specimens with a good shape and a smooth surface could be fabricated at a scan speed of 10 mm/s and a scan pitch of 0.6 mm.
- (2) A higher density and good microstructure of the sintered body could be obtained at a weight ratio of 4.
- (3) The tensile specimen could be successfully fabricated by investigation of laser-sintering conditions. The tensile strength and elongation of the sintered body were 280 MPa and 15% respectively.

### References

- [1] J.J. Beaman, J.W. Barlow, D.L. Bourell, R.H. Crawford, H.L. Marcus and K.P. McAlea, *Solid Freeform Fabrication: A New Direction in Manufacturing*, Kluwer Academic Publishers, Massachusetts, 1997.
- [2] D.L. Bourell, H.L. Marcus, J.W. Barlow and J.J. Beaman, "Selective laser sintering of metals and ceramics", *International Journal of Powder Metallurgy*, Vol.28, No.4, 1992, pp.369-381.
- [3] M.K. Agarwala, D.L. Bourell, J.J. Beaman, H.L. Marcus and J.W. Barlow, "Direct selective laser sintering of metals", *Rapid Prototyping Journal*, Vol.1, No.1, 1995, pp.26-36.
- [4] L. Lu, J. Fuh and Y.-S. Wong, *Laser-Induced materials and Processes for Rapid prototyping*, Kluwer Academic Publishers, Massachusetts, 2001.
- [5] F. Klocke, T. Celiker and Y.-A. Song, "Rapid metal tooling", *Rapid Prototyping Journal*, Vol.1, No.3, 1995, pp.32-42.
- [6] S. Das, M. Wohler, J.J. Beaman and D.L. Bourell, "Direct selective laser sintering of high performance metals for containerless HIP", *Advances in Powder Metallurgy & Particulate Materials-1997*, Part21, Compiled by R. A. McKotch and R. Webb, MPIF, New Jersey, 1997, pp.67-78.
- [7] Edited by J. R. Davis, *Metals Handbook Desk Edition, 2<sup>nd</sup> Ed.*, ASM International, Ohio, 1998, p.1081.
- [8] H. Kyogoku, S. Komatsu, H. Nakayama, H. Jinushi and K. Shinohara, "Microstructures and Mechanical Properties of Sintered Precipitation Hardening Stainless Steel Compacts by Metal Injection Molding", *Advances in Powder Metallurgy & Particulate Materials-1997*, Part18, Compiled by R. A. McKotch and R. Webb, MPIF, New Jersey, 1997, pp.135-144.